Equalization of OSDM over time-varying channels based on diagonal-block-banded matrix enhancement

Han, Jing; Wang, Yujie; Gong, Zehui; Leus, Geert

DOI
10.1016/j.sigpro.2019.107333

Publication date
2020

Document Version
Final published version

Published in
Signal Processing

Citation (APA)
Han, J., Wang, Y., Gong, Z., & Leus, G. (2020). Equalization of OSDM over time-varying channels based on diagonal-block-banded matrix enhancement. *Signal Processing*, *168*, 1-6. Article 107333. https://doi.org/10.1016/j.sigpro.2019.107333

Signal Processing 168 (2020) 107333

Contents lists available at ScienceDirect

Signal Processing

journal homepage: www.elsevier.com/locate/sigpro

Short communication

Equalization of OSDM over time-varying channels based on diagonal-block-banded matrix enhancement

Jing Han[a,*], Yujie Wang[a], Zehui Gong[a], Geert Leus[b]

[a] The School of Marine Science and Technology, Northwestern Polytechnical University, Xi'an, 710072, China
[b] The Faculty of Electrical Engineering, Mathematics and Computer Science, Delft University of Technology, Delft 2826 CD, The Netherlands

ARTICLE INFO

Article history:
Received 3 January 2019
Revised 1 October 2019
Accepted 7 October 2019
Available online 8 October 2019

Keywords:
OSDM
Time-varying channel
Inter-vector interference
Equalization
Underwater acoustic communication,

ABSTRACT

Orthogonal signal-division multiplexing (OSDM) has recently emerged as a promising alternative to orthogonal frequency division multiplexing (OFDM) for high-rate wireless communications. Although providing more flexibility in system design, it suffers from a special interference structure, namely inter-vector interference (IVI), when channel time variations are present. In this paper, we first derive the general OSDM signal model over time-varying channels, and then show that a time-domain window can be used to enhance the diagonal-block-banded (DBB) approximation of the channel matrix in a transformed domain. Furthermore, based on the DBB matrix enhancement, a low-complexity OSDM equalization algorithm is designed. Simulation results indicate that the proposed equalizer has significant performance advantages over that using the direct DBB approximation.

1. Introduction

Orthogonal signal-division multiplexing (OSDM) is a generalized modulation scheme which contains orthogonal frequency-division multiplexing (OFDM) and single-carrier block transmission (SCBT) as two extreme cases. Compared to the per-subcarrier modulation of OFDM in the frequency domain [1] and the per-sample modulation of SCBT in the time domain [2], OSDM modulation operates on segments of a block, termed as *vectors*, by which its symbol energy is distributed in both the time and frequency domains. Also, by selecting the length of these vectors, OSDM can enable a more flexible system design, and offer multiple tradeoffs between peak-to-average power ratio and granularity in bandwidth management.

OSDM was first proposed in [3,4] and has a similar signal structure as vector OFDM, which was developed in [5–7]. All these earlier works consider only time-invariant (TI) channels. More recently, due to its flexibility, OSDM has also been applied for underwater acoustic (UWA) communications [8–11], where the channels are typically time-varying (TV). It has been shown that the vectors in OSDM are a counterpart of the subcarriers in OFDM. Specifically, for the TI case, just like OFDM, which preserves the orthogonality of subcarriers, OSDM retains that of vectors [7]. Otherwise, when channel time variations are present, inter-vector interference (IVI) is induced in OSDM, which is analogous to inter-carrier interference (ICI) in OFDM [11].

In this paper, we focus on equalization of OSDM over TV channels. So far, the research on this issue is limited, and the existing methods are based on some simplified channel Doppler models. For instance, path-uniform Doppler models with a carrier frequency offset or a TV phase distortion are used in [10,11], respectively. These models assume a common Doppler effect on all channel paths, under which a phase compensation can be first performed, and then only a standard OSDM equalizer for TI channels is required. Moreover, by recognizing the risk of oversimplification in the path-uniform Doppler assumption, the complex exponential basis expansion model (CE-BEM) is adopted in [9,12] to accommodate more complex path-specific Doppler effects. It models the time variation on each channel delay tap independently by a few exponential functions, thus enabling more Doppler-resilient equalization. However, due to the modeling error of the CE-BEM, the OSDM equalization in this case may also suffer from a severe system performance loss.

The aim of this paper is to further improve the performance of OSDM equalization over TV channels. The main contributions can be summarized as follows.

- A general OSDM signal model over TV channels is derived. It shows that the composite channel matrix is normally a full matrix and the CE-BEM actually enforces a diagonal-block-banded (DBB) approximation on it in a transformed domain. To alleviate the system performance loss thus caused, a special time-

* Corresponding author..
E-mail addresses: hanj@nwpu.edu.cn (J. Han), yjwang@mail.nwpu.edu.cn (Y. Wang), gongzehui@mail.nwpu.edu.cn (Z. Gong), g.j.t.leus@tudelft.nl (G. Leus).

https://doi.org/10.1016/j.sigpro.2019.107333
0165-1684/

domain window is introduced, which can render the precision of the DBB approximation enhanced.
- A low-complexity OSDM equalization algorithm is designed accordingly based on the DBB matrix enhancement. It exploits the special matrix structure and uses the block LDL^H factorization to achieve a linear complexity in the transformed domain. Moreover, thanks to the enhanced DBB approximation of the channel matrix, it can significantly outperform the equalizer with a direct DBB approximation as done in [12].

The remainder of this paper is organized as follows. In Section 2, we derive the general OSDM signal model over TV channels. Based on that, in Section 3, we further describe the DBB matrix enhancement and the proposed OSDM equalization algorithm. The numerical simulation results are given in Section 4, and conclusions are drawn in Section 5.

Notation: $(\cdot)^*$ stands for conjugate, $(\cdot)^T$ for transpose, $(\cdot)^H$ for Hermitian transpose, $\|\cdot\|$ for the Frobenius norm, and $(\cdot)_K$ for the modulo-K operation. Moreover, $\otimes$ denotes the Kronecker product, and $\odot$ denotes the Hadamard (elementwise) product. We define $[\mathbf{x}]_n$ as the nth entry of the vector $\mathbf{x}$, and $[\mathbf{X}]_{m,n}$ as the (m, n)th entry of the matrix $\mathbf{X}$, where all indices are starting from 0. Similarly, $[\mathbf{x}]_{m:n}$ indicates the subvector of $\mathbf{x}$ from entry m to n, and $[\mathbf{X}]_{m:n,p:q}$ indicates the submatrix of $\mathbf{X}$ from row m to n and from column p to q, where only the colon is kept when all rows or columns are included. We use diag$\{\mathbf{x}\}$ to represent a diagonal matrix with $\mathbf{x}$ on its diagonal, and Diag$\{\mathbf{A}_0, \ldots, \mathbf{A}_{N-1}\}$ to represent a block-diagonal matrix created with the submatrices $\{\mathbf{A}_n\}_{n=0}^{N-1}$. Also, circ$\{\mathbf{x}\}$ is a circulant matrix whose first column is $\mathbf{x}$, and Circ$\{\mathbf{A}_0, \ldots, \mathbf{A}_{N-1}\}$ is a block-circulant matrix with its first block column being $[\mathbf{A}_0^T, \ldots, \mathbf{A}_{N-1}^T]^T$. Moreover, $\mathbf{F}_N$ stands for the $N \times N$ unitary discrete Fourier transform (DFT) matrix; $\mathbf{I}_N$ and $\mathbf{e}_N(n)$ refer to the $N \times N$ identity matrix and its nth column, respectively; $\mathbf{0}_N$ ($\mathbf{1}_N$) denotes the $N \times 1$ all-zero (all-one) vector.

2. Signal model

Let us start with a brief introduction of OSDM and compare it with conventional OFDM. We consider a data block $\mathbf{d}$ of $K = MN$ symbols. At the transmitter, conventional OFDM modulation is implemented by a single length-K inverse DFT (IDFT), i.e., $\mathbf{s} = \mathbf{F}_K^H \mathbf{d}$. In contrast, OSDM modulation is implemented by block interleaving and M IDFTs of length N, which can be expressed as [11]

$$\mathbf{s} = \left(\mathbf{F}_N^H \otimes \mathbf{I}_M\right)\mathbf{d}. \tag{1}$$

Then, after inserting a cyclic prefix (CP) of length longer than the channel impulse response (CIR), the OSDM signal is upconverted to the carrier frequency and transmitted through the channel.

Accordingly, at the receiver, by CP removal the inter-block interference is eliminated, and the resulting $K \times 1$ received block $\mathbf{r}$ can be generally modeled as

$$\mathbf{r} = \widetilde{\mathbf{C}}\mathbf{s} + \mathbf{n}, \tag{2}$$

where $\widetilde{\mathbf{C}}$ is the $K \times K$ channel matrix whose form depends on the specified channel model; $\mathbf{n}$ is the $K \times 1$ noise term. Likewise, in comparison with conventional OFDM demodulation, which is implemented by a single length-K DFT, i.e., $\mathbf{x} = \mathbf{F}_K \mathbf{r}$, OSDM demodulation is implemented by block interleaving and M DFTs of length N, i.e., the $K \times 1$ OSDM demodulated block is

$$\mathbf{x} = (\mathbf{F}_N \otimes \mathbf{I}_M)\mathbf{r} = \mathbf{C}\mathbf{d} + \mathbf{z}, \tag{3}$$

where $\mathbf{C} = (\mathbf{F}_N \otimes \mathbf{I}_M)\widetilde{\mathbf{C}}(\mathbf{F}_N^H \otimes \mathbf{I}_M)$ is termed as the composite channel matrix in this paper; $\mathbf{z} = (\mathbf{F}_N \otimes \mathbf{I}_M)\mathbf{n}$ is the demodulated noise.

From (1) and (3), it can be seen that OSDM is reduced to conventional OFDM when $M = 1$ and $N = K$; otherwise, OSDM will have a different signal model from OFDM. In the following, we first review the OSDM signal model over TI channels, based on which our emphasis is to establish a general OSDM signal model over TV channels.

2.1. TI channels

By defining the TI CIR vector as $\mathbf{c} = [c_0, c_1, \ldots, c_L]^T$, where L is the channel order, the channel matrix in (2) has the form

$$\widetilde{\mathbf{C}} = \text{circ}\{[\mathbf{c}^T, \mathbf{0}_{K-L-1}^T]^T\}. \tag{4}$$

It has been shown in [7,11] that, in this case,

$$\mathbf{C} = \text{Diag}\{\mathbf{C}_0, \mathbf{C}_1, \ldots, \mathbf{C}_{N-1}\}, \tag{5}$$

where, for $n = 0, 1, \ldots, N-1$,

$$\mathbf{C}_n = \mathbf{\Lambda}_M^{nH} \mathbf{F}_M^H \bar{\mathbf{C}}_n \mathbf{F}_M \mathbf{\Lambda}_M^n, \tag{6}$$

$$\mathbf{\Lambda}_M^n = \text{diag}\{[1, e^{-j\frac{2\pi n}{K}}, \ldots, e^{-j\frac{2\pi n}{K}(M-1)}]^T\}, \tag{7}$$

$$\bar{\mathbf{C}}_n = \text{diag}\left\{[h_n, h_{N+n}, \ldots, h_{(M-1)N+n}]^T\right\}, \tag{8}$$

and $h_i = \sum_{l=0}^{L} c_l e^{-j\frac{2\pi}{K}li}$ for $i = 0, 1, \ldots, K-1$.

We can see that $\mathbf{C}$ in (5) is a block-diagonal matrix. By partitioning the $K \times 1$ blocks $\mathbf{d}$, $\mathbf{x}$ and $\mathbf{z}$ into N vectors of length M, and defining $\mathbf{d}_n = [\mathbf{d}]_{nM:nM+M-1}$, $\mathbf{x}_n = [\mathbf{x}]_{nM:nM+M-1}$ and $\mathbf{z}_n = [\mathbf{z}]_{nM:nM+M-1}$ as the nth symbol vector, demodulated vector and noise vector, respectively, it can be obtained that

$$\mathbf{x}_n = \mathbf{C}_n \mathbf{d}_n + \mathbf{z}_n. \tag{9}$$

This means that, over a TI channel, different from conventional OFDM which can decouple all K tones at the receiver, OSDM preserves orthogonality among its N vectors. In other words, the inter-symbol interference (ISI) of OSDM in this case is confined within each vector.

2.2. TV channels

In this paper, we consider the TV channel case. Here, the channel is directly modeled by the TV CIR $\{c_{k,l}\}$, where k and l are the time and delay indices, respectively. And the channel matrix in (2) has entries

$$[\widetilde{\mathbf{C}}]_{k,k'} = c_{k,(k-k')_K}, \tag{10}$$

for $0 \le k, k' \le K-1$.

To derive the structure of $\mathbf{C}$ in this case, we use the fact that the DFT matrix of dimension $K = MN$ can be factorized into [12]

$$\mathbf{F}_K = \mathbf{P}_{N,M}(\mathbf{I}_N \otimes \mathbf{F}_M)\mathbf{\Lambda}(\mathbf{F}_N \otimes \mathbf{I}_M), \tag{11}$$

where $\mathbf{\Lambda} = \text{Diag}\{\mathbf{\Lambda}_M^0, \mathbf{\Lambda}_M^1, \ldots, \mathbf{\Lambda}_M^{N-1}\}$, and $\mathbf{P}_{N,M}$ is the $K \times K$ permutation matrix defined as

$$\mathbf{P}_{N,M} = \begin{bmatrix} \mathbf{I}_N \otimes \mathbf{e}_M^T(0) \\ \mathbf{I}_N \otimes \mathbf{e}_M^T(1) \\ \vdots \\ \mathbf{I}_N \otimes \mathbf{e}_M^T(M-1) \end{bmatrix}. \tag{12}$$

Based on (11) and the Kronecker product property, i.e., $(\mathcal{A}_1 \otimes \mathcal{B}_1)(\mathcal{A}_2 \otimes \mathcal{B}_2) = (\mathcal{A}_1\mathcal{A}_2) \otimes (\mathcal{B}_1\mathcal{B}_2)$, it can be obtained that

$$\begin{aligned} \mathbf{C} &= \left[(\mathbf{F}_N \otimes \mathbf{I}_M)\mathbf{F}_K^H\right]\bar{\mathbf{B}}\left[\mathbf{F}_K\left(\mathbf{F}_N^H \otimes \mathbf{I}_M\right)\right] \\ &= \left[\mathbf{\Lambda}^H\left(\mathbf{I}_N \otimes \mathbf{F}_M^H\right)\right]\bar{\mathbf{C}}[(\mathbf{I}_N \otimes \mathbf{F}_M)\mathbf{\Lambda}], \end{aligned} \tag{13}$$

where $\bar{\mathbf{B}} = \mathbf{F}_K \widetilde{\mathbf{C}} \mathbf{F}_K^H$ and $\bar{\mathbf{C}} = \mathbf{P}_{N,M}^H \bar{\mathbf{B}} \mathbf{P}_{N,M}$.

We know that $\bar{\mathbf{B}}$ in (13) is the channel Doppler-frequency response matrix. It has entries $[\bar{\mathbf{B}}]_{i,i'} = b_{i-i',i'}$ with

$$b_{q,i} = \frac{1}{K}\sum_{k=0}^{K-1}\sum_{l=0}^{L} c_{k,l} e^{-j\frac{2\pi}{K}(li+kq)}, \tag{14}$$

where q and i are the Doppler and frequency indices, respectively [13]. As such, the matrix $\mathbf{C}$ in this case is no longer block-diagonal. By partitioning it into $M \times M$ blocks

$$\mathbf{C}_{n,n'} = [\mathbf{C}]_{nM:nM+M-1,n'M:n'M+M-1}, \tag{15}$$

for $0 \le n, n' \le N-1$, and plugging it into (3), the nth OSDM demodulated vector has the form

$$\mathbf{x}_n = \mathbf{C}_{n,n}\mathbf{d}_n + \sum_{n' \ne n} \mathbf{C}_{n,n'}\mathbf{d}_{n'} + \mathbf{z}_n. \tag{16}$$

Here, on the right-hand side of (16), the second term represents the IVI, which is analogous to the ICI in conventional OFDM. It means that, over a TV channel, orthogonality among the N vectors in OSDM is destroyed.

3. Channel equalization

3.1. Channel matrix structure

To achieve low-complexity equalization of OSDM over TV channels, let us further examine the matrix structures of $\bar{\mathbf{B}}$ and $\bar{\mathbf{C}}$. It can be observed that $\{b_{q,i}\}$ are stored (cyclically) along diagonals in $\bar{\mathbf{B}}$. To be specific, the Doppler index $q = 0$ corresponds to the main diagonal, while $q > 0$ ($q < 0$) corresponds to the qth lower (upper) diagonal. Then, by pre- and post-multiplying by $\mathbf{P}_{N,M}^H$ and $\mathbf{P}_{N,M}$, the matrix $\bar{\mathbf{C}}$ performs interleaving on $\bar{\mathbf{B}}$ along rows and columns, respectively.

Since the TV CIR $\{c_{k,l}\}$ is typically slow-varying, we first consider a simple case where $\{b_{q,i}\}$ is strictly band-limited in the Doppler domain. Assuming that $b_{q,i} = 0$ for $q < -Q$ and $q > Q$, we have that $\bar{\mathbf{B}}$ in this case is a (cyclically) scalar-banded matrix. Then, by further introducing the assumption that $Q < N/2$, after permutation, $\bar{\mathbf{C}}$ is (cyclically) block-banded with block size $M \times M$ and block semi-bandwidth (BSB) Q. To provide some intuition, an example of $\bar{\mathbf{B}}$ and $\bar{\mathbf{C}}$ is illustrated in Fig. 1.

This matrix structure implies that IVI comes only from the neighboring $2Q$ vectors. Moreover, it can be obtained that all blocks in the main block band (except the bottom-left and top-right corners) of $\bar{\mathbf{C}}$ are diagonal. We can easily have

$$\bar{\mathbf{C}}_{n,n'} = \mathrm{diag}\{[b_{n-n',n'}, b_{n-n',n'+N}, \ldots, b_{n-n',n'+(M-1)N}]^T\}, \tag{17}$$

for $|n - n'| \le Q$, where $\bar{\mathbf{C}}_{n,n'}$ is the (n, n')th block of $\bar{\mathbf{C}}$ defined similarly as (15).

Furthermore, to remove the nondiagonal blocks in the two corners, we place $2Q$ zero vectors at the edges of the transmitted data block, i.e., $\mathbf{d} = [\mathbf{0}_{QM}^T, \underline{\mathbf{d}}^T, \mathbf{0}_{QM}^T]^T$ and $\underline{\mathbf{d}}$ contains $\underline{N} = N - 2Q$ vectors. Accordingly, at the OSDM receiver, we extract the central $\underline{N}$ vectors in the block to obtain $\underline{\mathbf{x}} = \mathbf{T}\mathbf{x}$, where $\mathbf{T} = [\mathbf{I}_K]_{QM:(N-Q)M-1,:}$. Based on (3) and (13), the signal model in this case can be rewritten as

$$\begin{aligned}\underline{\mathbf{x}} &= \underline{\mathbf{C}}\underline{\mathbf{d}} + \underline{\mathbf{z}} \\ &= \left[\underline{\mathbf{\Lambda}}^H(\mathbf{I}_{\underline{N}} \otimes \mathbf{F}_M^H)\right]\bar{\underline{\mathbf{C}}}\left[(\mathbf{I}_{\underline{N}} \otimes \mathbf{F}_M)\underline{\mathbf{\Lambda}}\right]\underline{\mathbf{d}} + \underline{\mathbf{z}},\end{aligned} \tag{18}$$

where $\underline{\mathbf{C}} = \mathbf{T}\mathbf{C}\mathbf{T}^H$, $\bar{\underline{\mathbf{C}}} = \mathbf{T}\bar{\mathbf{C}}\mathbf{T}^H$, $\underline{\mathbf{z}} = \mathbf{T}\mathbf{z}$ and $\underline{\mathbf{\Lambda}} = \mathrm{Diag}\{\mathbf{\Lambda}_M^Q, \mathbf{\Lambda}_M^{Q+1}, \ldots, \mathbf{\Lambda}_M^{N-Q-1}\}$. Note that, after the truncation, the resulting matrix $\bar{\underline{\mathbf{C}}}$ in (18) is block-banded (not cyclically) with BSB $\beta_{\mathrm{C}} = \min\{Q, \underline{N} - 1\}$ and all its nonzero blocks are diagonal. This matrix structure is termed to be DBB in this paper, which is fundamental to enable low-complexity equalization of OSDM over TV channels (see Section 3.3 for details).

However, we should also note that in practice the channel assumption of limited Doppler spread would not be perfectly satisfied. As a result, $\bar{\underline{\mathbf{C}}}$ is in general not block-banded and its blocks are actually not diagonal.

3.2. DBB matrix enhancement

In our previous work [12], the CE-BEM is used to model the TV channel, and its CIR is approximated by

$$c_{k,l} = \sum_{q=-Q}^{Q} h_{q,l} e^{j\frac{2\pi}{K}kq}, \tag{19}$$

where $Q < N/2$ represents the Doppler spread, and $h_{q,l}$ is the BEM coefficient at Doppler index q and delay index l. It can be seen that the TV CIR is here modeled by a superposition of $2Q+1$ complex exponential basis functions, which enforces the limited Doppler spread assumption in Section 3.1. Then, based on (14), we can write

$$b_{q,i} = \sum_{l=0}^{L} h_{q,l} e^{-j\frac{2\pi}{K}li}, \tag{20}$$

for $|q| \le Q$, and $b_{q,i} = 0$ otherwise. In this case, the matrix $\bar{\underline{\mathbf{C}}}$ is actually replaced by its direct DBB approximation

$$\overline{\underline{\mathbb{C}}} = \bar{\underline{\mathbf{C}}} \odot \mathbf{M}_{\mathrm{C}}, \tag{21}$$

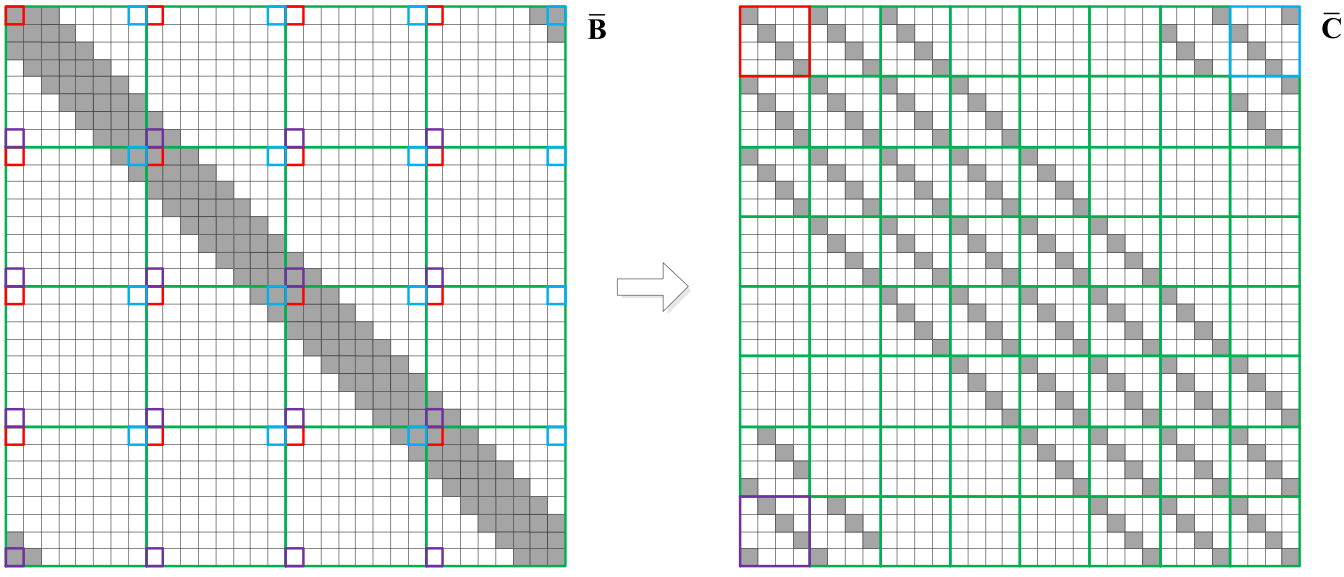

Fig. 1. An example of the matrix structures of $\bar{\mathbf{B}}$ and $\bar{\mathbf{C}}$ with $M = 4$, $N = 8$ and $Q = 2$.

where $\mathbf{M}_{\mathrm{C}}$ is the DBB mask matrix, i.e., 1-valued on the block diagonals within the main block band and 0-valued elsewhere. However, nulling entries of $\bar{\underline{\mathbf{C}}}$ directly as in (21) may sometimes lead to a large channel approximation error.

To counteract this problem, a time-domain window is introduced at the OSDM receiver to enhance the DBB approximation of the matrix $\bar{\underline{\mathbf{C}}}$. We denote the length-$K$ receiver window with $\widetilde{\mathbf{W}} = \mathrm{diag}\{\mathbf{w}\}$. Compared to (2), the windowed version of the received block is

$$\mathbf{r}_{\mathrm{w}} = \widetilde{\mathbf{C}}_{\mathrm{w}}\mathbf{s} + \mathbf{n}_{\mathrm{w}}, \tag{22}$$

where $\mathbf{r}_{\mathrm{w}} = \widetilde{\mathbf{W}}\mathbf{r}$, $\mathbf{n}_{\mathrm{w}} = \widetilde{\mathbf{W}}\mathbf{n}$ and $\widetilde{\mathbf{C}}_{\mathrm{w}} = \widetilde{\mathbf{W}}\widetilde{\mathbf{C}}$. Furthermore, by similarly defining $\mathbf{C}_{\mathrm{w}} = (\mathbf{F}_N \otimes \mathbf{I}_M)\widetilde{\mathbf{C}}_{\mathrm{w}}(\mathbf{F}_N^H \otimes \mathbf{I}_M)$, $\bar{\mathbf{B}}_{\mathrm{w}} = \mathbf{F}_K\widetilde{\mathbf{C}}_{\mathrm{w}}\mathbf{F}_K^H$ and $\bar{\mathbf{C}}_{\mathrm{w}} = \mathbf{P}_{N,M}^H\bar{\mathbf{B}}_{\mathrm{w}}\mathbf{P}_{N,M}$ as in (3) and (13), we can repeat the derivation in (18) and obtain

$$\begin{aligned}\underline{\mathbf{x}}_{\mathrm{w}} &= \underline{\mathbf{C}}_{\mathrm{w}}\underline{\mathbf{d}} + \underline{\mathbf{z}}_{\mathrm{w}} \\ &= \left[\underline{\mathbf{\Lambda}}^H(\mathbf{I}_{\underline{N}} \otimes \mathbf{F}_M^H)\right]\bar{\underline{\mathbf{C}}}_{\mathrm{w}}\left[(\mathbf{I}_{\underline{N}} \otimes \mathbf{F}_M)\underline{\mathbf{\Lambda}}\right]\underline{\mathbf{d}} + \underline{\mathbf{z}}_{\mathrm{w}},\end{aligned} \tag{23}$$

where $\underline{\mathbf{C}}_{\mathrm{w}} = \mathbf{T}\mathbf{C}_{\mathrm{w}}\mathbf{T}^H$, $\bar{\underline{\mathbf{C}}}_{\mathrm{w}} = \mathbf{T}\bar{\mathbf{C}}_{\mathrm{w}}\mathbf{T}^H$ and $\underline{\mathbf{z}}_{\mathrm{w}} = \mathbf{T}(\mathbf{F}_N \otimes \mathbf{I}_M)\mathbf{n}_{\mathrm{w}}$.

To achieve an enhanced DBB approximation of $\bar{\underline{\mathbf{C}}}_{\mathrm{w}}$ (compared to the unwindowed version $\bar{\underline{\mathbf{C}}}$), the optimum window can be computed by solving

$$\max_{\mathbf{w}} \left\|\bar{\underline{\mathbf{C}}}_{\mathrm{w}} \odot \mathbf{M}_{\mathrm{C}}\right\|^2, \qquad \text{s.t.} \quad \mathbf{w}^H\mathbf{w} = N. \tag{24}$$

Moreover, due to the permutation relationship between $\bar{\mathbf{B}}_{\mathrm{w}}$ and $\bar{\mathbf{C}}_{\mathrm{w}}$, the optimization problem in (24) can be approximately reformulated as

$$\max_{\mathbf{w}} \left\|\bar{\mathbf{B}}_{\mathrm{w}} \odot \mathbf{M}_{\mathrm{B}}\right\|^2, \qquad \text{s.t.} \quad \mathbf{w}^H\mathbf{w} = N, \tag{25}$$

where $\mathbf{M}_{\mathrm{B}} = \mathrm{circ}\{[\mathbf{1}_{Q+1}^T, \mathbf{0}_{K-2Q-1}^T, \mathbf{1}_Q^T]^T\}$ is the corresponding scalar-banded mask matrix.

We here adopt the minimum band-approximation-error sum-of-exponentials (MBAE-SOE) window design strategy in [14], which models $\mathbf{w}$ as a sum of exponentials, i.e.,

$$\mathbf{w} = [\mathbf{f}_{-Q}, \ldots, \mathbf{f}_0, \ldots, \mathbf{f}_Q]\mathbf{a}, \tag{26}$$

where $\mathbf{f}_q = [1, e^{j\frac{2\pi q}{K}}, \ldots, e^{j\frac{2\pi q}{K}(K-1)}]^T$ for $q = -Q, \ldots Q$, and $\mathbf{a} = [a_{-Q}, \ldots, a_0, \ldots, a_Q]^T$ is the coefficient vector. With this model, a similar approach as in [13,14] can be used to obtain an optimum window for the problem (24). It squeezes the significant coefficients of $\bar{\underline{\mathbf{C}}}_{\mathrm{w}}$ into the entries indicated by $\mathbf{M}_{\mathrm{C}}$ and thus achieves an enhanced DBB structure.

3.3. Equalization algorithm

Different from the algorithms in [12], the channel equalization of OSDM in this paper has to deal with colored noise. Specifically, assuming that $\mathbf{n}$ in (2) is additive white Gaussian noise with entries of zero mean and variance σ^2, we have $E\{\mathbf{z}\mathbf{z}^H\} = E\{\mathbf{n}\mathbf{n}^H\} = \sigma^2\mathbf{I}_K$. However, due to the receiver windowing, $\underline{\mathbf{z}}_{\mathrm{w}}$ in (23) is colored with covariance matrix

$$\underline{\mathbf{\Pi}}_{\mathrm{w}} = E\left\{\underline{\mathbf{z}}_{\mathrm{w}}\underline{\mathbf{z}}_{\mathrm{w}}^H\right\} = \sigma^2\mathbf{T}\mathbf{W}\mathbf{W}^H\mathbf{T}^H, \tag{27}$$

where $\mathbf{W} = (\mathbf{F}_N \otimes \mathbf{I}_M)\widetilde{\mathbf{W}}(\mathbf{F}_N^H \otimes \mathbf{I}_M)$. And, similar to (13), we can obtain that

$$\begin{aligned}\mathbf{W} &= \left[(\mathbf{F}_N \otimes \mathbf{I}_M)\mathbf{F}_K^H\right]\bar{\mathbf{V}}\left[\mathbf{F}_K\left(\mathbf{F}_N^H \otimes \mathbf{I}_M\right)\right] \\ &= \left[\mathbf{\Lambda}^H\left(\mathbf{I}_N \otimes \mathbf{F}_M^H\right)\right]\bar{\mathbf{W}}[(\mathbf{I}_N \otimes \mathbf{F}_M)\mathbf{\Lambda}],\end{aligned} \tag{28}$$

where $\bar{\mathbf{V}} = \mathbf{F}_K\widetilde{\mathbf{W}}\mathbf{F}_K^H$ and $\bar{\mathbf{W}} = \mathbf{P}_{N,M}^H\bar{\mathbf{V}}\mathbf{P}_{N,M}$. Thus, by further defining $\bar{\underline{\mathbf{W}}} = \mathbf{T}\bar{\mathbf{W}}$, (27) can be rewritten as

$$\underline{\mathbf{\Pi}}_{\mathrm{w}} = \sigma^2\left[\underline{\mathbf{\Lambda}}^H(\mathbf{I}_{\underline{N}} \otimes \mathbf{F}_M^H)\right]\bar{\underline{\mathbf{W}}}\bar{\underline{\mathbf{W}}}^H\left[(\mathbf{I}_{\underline{N}} \otimes \mathbf{F}_M)\underline{\mathbf{\Lambda}}\right]. \tag{29}$$

We now assume that the symbols in $\underline{\mathbf{d}}$ are independent and identically distributed with unit power, i.e., $E\{\underline{\mathbf{d}}\underline{\mathbf{d}}^H\} = \mathbf{I}_{M\underline{N}}$. Then, from (23) and (27), a straightforward minimum mean-square error (MMSE) block equalizer can be expressed as

$$\widehat{\underline{\mathbf{d}}} = \underline{\mathbf{C}}_{\mathrm{w}}^H\left(\underline{\mathbf{C}}_{\mathrm{w}}\underline{\mathbf{C}}_{\mathrm{w}}^H + \underline{\mathbf{\Pi}}_{\mathrm{w}}\right)^{-1}\underline{\mathbf{x}}_{\mathrm{w}}, \tag{30}$$

where $\widehat{\underline{\mathbf{d}}}$ is the estimate of $\underline{\mathbf{d}}$. Due to the matrix inversion, direct computation of (30) incurs a complexity of $\mathcal{O}(K^3)$.

To achieve a low-complexity equalization algorithm, we alternatively use the matrix factorizations in (23) and (29). Moreover, since $\bar{\underline{\mathbf{C}}}_{\mathrm{w}}$ has an enhanced DBB structure, we can approximate it by $\bar{\underline{\mathbb{C}}}_{\mathrm{w}} = \bar{\underline{\mathbf{C}}}_{\mathrm{w}} \odot \mathbf{M}_{\mathrm{C}}$. The channel equalization in this case can be rewritten as

$$\widehat{\underline{\mathbf{d}}} = \left[\underline{\mathbf{\Lambda}}^H(\mathbf{I}_{\underline{N}} \otimes \mathbf{F}_M^H)\right]\bar{\underline{\mathbb{C}}}_{\mathrm{w}}^H\bar{\underline{\mathbf{R}}}_{\mathrm{w}}^{-1}\left[(\mathbf{I}_{\underline{N}} \otimes \mathbf{F}_M)\underline{\mathbf{\Lambda}}\right]\underline{\mathbf{x}}_{\mathrm{w}}, \tag{31}$$

where $\bar{\underline{\mathbf{R}}}_{\mathrm{w}} = \bar{\underline{\mathbb{C}}}_{\mathrm{w}}\bar{\underline{\mathbb{C}}}_{\mathrm{w}}^H + \sigma^2\bar{\underline{\mathbf{W}}}\bar{\underline{\mathbf{W}}}^H$ is a DBB matrix with BSB $\beta_{\mathrm{R}} = \min\{2Q, \underline{N} - 1\}$. This is because $\bar{\underline{\mathbb{C}}}_{\mathrm{w}}\bar{\underline{\mathbb{C}}}_{\mathrm{w}}^H$ is DBB with BSB β_{R}. On the other hand, based on the receiver window modeled in (26), we can easily obtain that $\bar{\mathbf{V}} = \mathrm{circ}\{[a_0, \ldots, a_Q, \mathbf{0}_{K-2Q-1}^T, a_{-Q}, \ldots, a_{-1}]^T\}$, and thus $\bar{\underline{\mathbf{W}}}\bar{\underline{\mathbf{W}}}^H$ is also DBB with BSB β_{R}.

Actually, (31) can be interpreted as a transformed-domain channel equalization algorithm. Here, the transform and its inverse are implemented by premultiplying with $(\mathbf{I}_{\underline{N}} \otimes \mathbf{F}_M)\underline{\mathbf{\Lambda}}$ and its Hermitian transpose, respectively. We can see that each direction of the transform involves a frequency (un)shifting operation and $\underline{N}$ (I)DFTs of size M. Accordingly, channel equalization in this case is performed not directly on $\underline{\mathbf{x}}_{\mathrm{w}}$ as in (30), but on its transformed version. Given the DBB structure of $\bar{\underline{\mathbf{R}}}_{\mathrm{w}}$, we can use the block LDL^H factorization as in [12] to invert it, and the OSDM equalization algorithm requires only a complexity of $\mathcal{O}(K)$ in the transformed domain.

4. Numerical simulations

In this section, numerical simulation results are provided to illustrate the performance improvement achieved by using the DBB matrix enhancement and its corresponding equalization algorithm in an OSDM system. We here adopt a similar UWA communication scenario as in [12], where OSDM blocks are composed of $K = 1024$ quaternary phase-shift keying (QPSK) symbols with symbol period $T_{\mathrm{s}} = 0.25$ ms, and thus the block duration is $T = KT_{\mathrm{s}} = 256$ ms. The doubly-selective channel is assumed to be Rayleigh distributed with uniform power delay profile and U-shaped Doppler spectrum. Specifically, the channel memory length is set to $L = 24$, which corresponds to a multipath delay spread of $\tau_{\max} = LT_{\mathrm{s}} = 6$ ms, while the channel time variation is parameterized by its maximum Doppler spread f_d. Moreover, since OSDM can actually be deemed as a precoded version of OFDM with subcarrier spacing $1/T$ [11], in the following simulations we use the normalized Doppler spread f_dT.

Fig. 2 shows the performance of the DBB matrix enhancement method. The quality of the DBB approximation is measured by its normalized mean-square error (NMSE)

$$\mathrm{NMSE} = \mathrm{E}\left\{\left\|\bar{\underline{\mathbf{C}}}_{\mathrm{w}} \odot \breve{\mathbf{M}}_{\mathrm{C}}\right\|^2\right\} / \mathrm{E}\left\{\left\|\bar{\underline{\mathbf{C}}}_{\mathrm{w}}\right\|^2\right\}, \tag{32}$$

where $\breve{\mathbf{M}}_{\mathrm{C}}$ is the complement of $\mathbf{M}_{\mathrm{C}}$, and $\mathrm{E}\{\cdot\}$ stands for the expectation operation. As stated in Section 3.2, the direct DBB approximation masks the channel matrix straightforwardly according to (21), while the enhanced DBB approximation first imposes the MBAE-SOE window computed in (24) and (26) on the received block. Here, the vector length is fixed to $M = 4$, and the normalized Doppler spread f_dT is generated in the range [0.1, 0.5]. It is easy to verify from (26) that, when $Q = 0$, the MBAE-SOE window reduces to a rectangular one, and thus the enhanced and direct DBB approximations are equivalent. However, as Q increases to

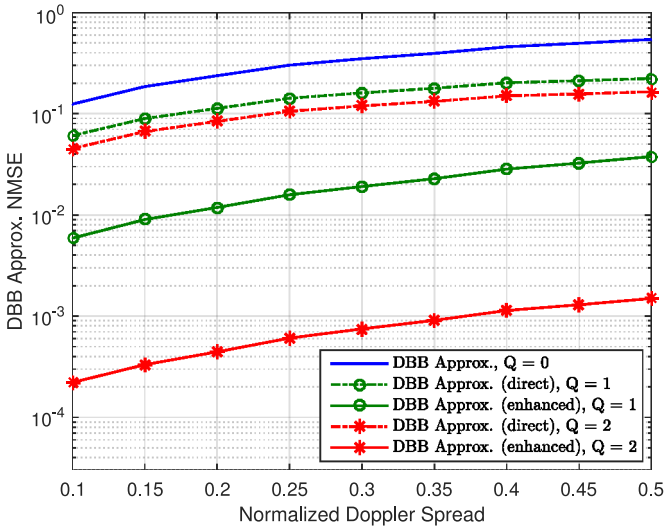

Fig. 2. NMSE performance comparison of the direct and enhanced DBB approximations.

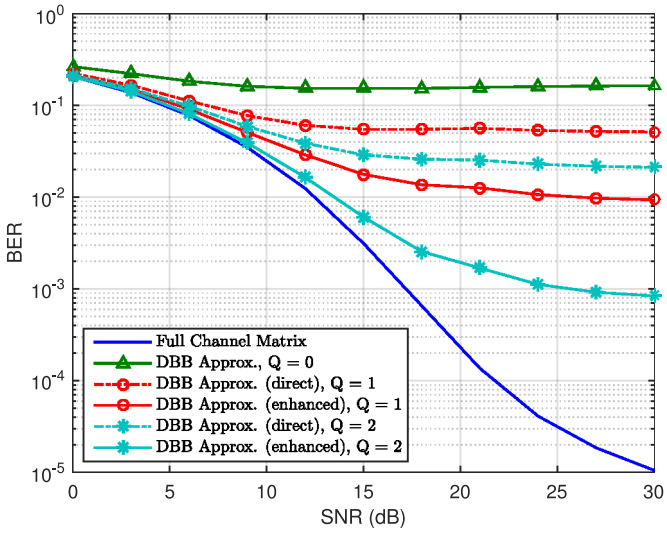

Fig. 3. BER performance of the proposed OSDM equalization algorithm as a function of the SNR with $M = 4$ and $f_dT = 0.5$.

1 and 2, the NMSE of the enhanced DBB approximation becomes much lower than that of direct masking. We can thus sparsify $\bar{\mathbf{C}}_{\mathrm{w}}$ by its DBB approximation $\overline{\mathbb{C}}_{\mathrm{w}}$ with more accuracy, which enables the design of low-complexity OSDM equalization.

Furthermore, Figs. 3 and 4 present the bit error rate (BER) performance of the proposed low-complexity OSDM equalization algorithm. Specifically, in Fig. 3, we fix $M = 4$ and $f_dT = 0.5$, and evaluate the performance as a function of the signal-to-noise ratio (SNR) for various Q values. It can be seen that, when $Q = 0$, all entries off the main diagonal of $\bar{\mathbf{C}}_{\mathrm{w}}$ are ignored and the channel is actually treated as TI, which leads to the highest BER. On the other hand, by using the full channel matrix, i.e., without any DBB approximation, the lowest BER is achieved. However, since no special matrix structure is now available, we can only resort to the direct equalization in (30) which has a cubic complexity. Bounded by these two extreme cases, the equalization performance is always better with the enhanced DBB approximation and the error floor improves as Q increases. These observations can be attributed to the corresponding NMSE results shown in Fig. 2.

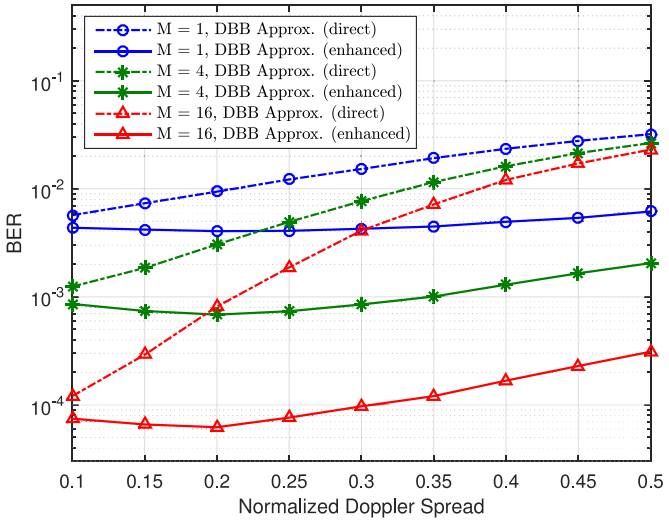

Fig. 4. BER performance of the proposed OSDM equalization algorithm as a function of the normalized Doppler spread with SNR = 20 dB and $Q = 2$.

In addition, in Fig. 4, we fix SNR = 20 dB and $Q = 2$, and evaluate the equalization performance as a function of the normalized Doppler spread for various vector lengths $M = 1$ (i.e., OFDM), 4 and 16. It can be seen that the BER performance benefits from a larger M. This is because OSDM can implicitly offer an intra-vector frequency diversity and its order generally increases with the vector length [7,11]. However, as f_dT increases, the direct DBB approximation gets worse quickly. The IVI and (intra-vector) ISI caused by the masked entries in $\bar{\mathbf{C}}_{\mathrm{w}}$ become no longer negligible. As a result, the OSDM system suffers a large performance degradation in this case, and the gaps among the BER curves for different M values are much narrower at high Doppler spreads. In contrast, by using the enhanced DBB approximation, the leakage of IVI and ISI can be significantly reduced, and the proposed OSDM equalization algorithm can mitigate the Doppler-induced performance loss effectively.

5. Conclusion

An equalization algorithm for OSDM is proposed in this paper to counteract the doubly-selective fading over TV channels. It offers two appealing features: 1) the algorithm is performed in a transformed domain and thus can achieve a low complexity (by using the block LDL^H factorization); 2) the algorithm is based on DBB matrix enhancement (by imposing the MBAE-SOE window) and thus can significantly improve the system performance compared to that using a direct DBB approximation.

Declaration of Competing Interest

The authors declare that they have no known competing financial interests or personal relationships that could have appeared to influence the work reported in this paper.

Acknowledgments

This work was supported in part by the National Natural Science Foundation of China under grants 61771394, 61531015, and 61801394, in part by the Natural Science Basic Research Plan in Shaanxi Province of China under grant 2018JM6042, in part by the 111 Project under grant B18041, and in part by the Seed Foundation of Innovation and Creation for Graduate Students in NWPU under grant ZZ2019006.

References

[1] T. Hwang, C. Yang, G. Wu, S. Li, G. Li, OFDM and its wireless applications: a survey, IEEE Trans. Veh. Technol. 58 (4) (2009) 1673–1694.

[2] F. Pancaldi, G. Vitetta, R. Kalbasi, N. Al-Dhahir, M. Uysal, H. Mheidat, Single-carrier frequency domain equalization, IEEE Commun. Mag. 25 (5) (2008) 37–56.

[3] N. Suehiro, C. Han, T. Imoto, N. Kuroyanagi, An information transmission method using Kronecker product, in: Proc. IASTED Int. Conf. Commun. Syst. Netw., 2002, pp. 206–209.

[4] N. Suehiro, C. Han, T. Imoto, Very efficient wireless frequency usage based on pseudo-coherent addition of multipath signals using Kronecker product with rows of DFT matrix, in: Proc. Int. Symp. Inf. Theory, 2003. pp. 385–385.

[5] X.G. Xia, Precoded OFDM systems robust to spectral null channels and vector OFDM systems with reduced cyclic prefix length, in: Proc. Int. Conf. Commun. (ICC), 2000, pp. 1110–1114.

[6] X.G. Xia, Precoded and vector OFDM robust to channel spectral nulls and with reduced cyclic prefix length in single transmit antenna systems, IEEE Trans. Commun. 49 (8) (2001) 1363–1374.

[7] Y. Li, I. Ngebani, X.-G. Xia, A. Host-Madsen, On performance of vector OFDM with linear receivers, IEEE Trans. Signal Process. 60 (10) (2012) 5268–5280.

[8] T. Ebihara, K. Mizutani, Underwater acoustic communication with an orthogonal signal division multiplexing scheme in doubly spread channels, IEEE J. Ocean. Eng. 39 (1) (2014) 47–58.

[9] T. Ebihara, G. Leus, Doppler-resilient orthogonal signal-division multiplexing for underwater acoustic communication, IEEE J. Ocean. Eng. 41 (2) (2016) 408–427.

[10] J. Han, W. Shi, G. Leus, Space-frequency coded orthogonal signal-division multiplexing over underwater acoustic channels, J. Acoust. Soc. Amer. 141 (6) (2017) EL513–EL518.

[11] J. Han, S. Chepuri, Q. Zhang, G. Leus, Iterative per-vector equalization for orthogonal signal-division multiplexing over time-varying underwater acoustic channels, IEEE J. Ocean. Eng. 44 (1) (2019) 240–255.

[12] J. Han, L. Zhang, Q. Zhang, G. Leus, Low-complexity equalization of orthogonal signal-division multiplexing in doubly-selective channels, IEEE Trans. Signal Process. 67 (4) (2019) 915–929.

[13] P. Schniter, Low-complexity equalization of OFDM in doubly selective channels, IEEE Trans. Signal Process. 52 (4) (2004) 1002–1011.

[14] L. Rugini, P. Banelli, G. Leus, Low-complexity banded equalizers for OFDM systems in Doppler spread channels, EURASIP J. Appl. Signal Process. 2006 (2006) 1–13. Article ID 67 404.